Raman Spectrosopic Characterization of Isomers of Copper and Zinc *N*-Phenylprotoporphyrin IX Dimethyl Ester

Laurie D. Sparks,[†,‡] James R. Chamberlain,[†] Pam Hsu,[‡] Mark R. Ondrias,[‡] Barbara A. Swanson,[§] Paul R. Ortiz de Montellano,[*,§] and John A. Shelnutt[*,†,‡]

Fuel Science Department 6211, Sandia National Laboratories, Albuquerque, New Mexico 87185, Department of Chemistry, University of New Mexico, Albuquerque, New Mexico 87131, and Department of Pharmaceutical Chemistry, School of Pharmacy, University of California, San Francisco, California 94143-0446

Received December 9, 1992

The reaction of certain heme-containing proteins with phenylhydrazine results in *N*-phenylprotoporphyrin formation. N-substituted porphyrins are known to inhibit ferrochelatase and to be formed in the inactivation of hepatic cytochrome P_{450} by various agents. These molecules therefore play an important role in understanding the biological function of these enzymes. We have used molecular modeling in conjunction with resonance Raman and UV–visible absorption spectroscopies to investigate the structure of the four distal regioisomers of *N*-phenylprotoporphyrin IX dimethyl ester (NPhPPDME) metal derivatives. Regardless of which pyrrole ring (A, B, C, or D) bears the *N*-phenyl substituent, a novel distortion from planarity of the protoporphyrin macrocycle results from addition of the phenyl group. The molecular mechanics calculations for various isomers and conformers of copper(II) *N*-phenylprotoporphyrin IX predict structures similar to the structure reported for zinc *N*-phenyltetraphenylporphyrin (Kuila, D.; et al. *J. Am. Chem Soc.* **1984**, *106*, 448), with the major distortion from planarity occurring for the N-substituted pyrrole ring. Although the four isomers of CuNPhPPDME are all similar when contrasted with CuPPDME, closer examination of the vibrational structure allowed the isomers to be separated into two groups. Differences among pairs of isomers are apparent primarily in the vinyl vibrational modes and vinyl-sensitive porphyrin modes. Even more subtle spectral differences distinguish all of the isomers. We present arguments suggesting that the spectral characteristics are the result of electronic rather than kinematic effects.

Introduction

The cytochromes P_{450} are physiologically important detoxifying agents. The function of certain hepatic cytochromes P_{450} is to catalyze the hydroxylation of various organic substrates and foreign substances, allowing more efficient elimination of these toxins from the body. The reaction of several xenobiotics, such as prescription drugs and anaesthetics, with cytochrome P_{450} produces an N-substituted porphyrin and hence a deactivated or catalytically inactive enzyme.[1] N-substituted porphyrins are also known to inhibit the enzyme ferrochelatase, the final enzyme in the heme biosynthetic pathway. Understanding the details of formation and structure of the *N*-phenylprotoporphyrin IX (NPhPP) suicide product aids in elucidating the mechanism of cytochrome P_{450} or ferrochelatase function.

Naturally produced N-substituted porphyrins (*N*-methylprotoporphyrins) isolated from the livers of drug-treated rats[2] were first characterized by Ortiz de Montellano and Kunze.[3] The N-substituted porphyrins originated from the reaction of 4-methyl-3,5-dihydrocollidine with a cytochrome P_{450} enzyme in the livers of the rodents. N-substituted porphyrins also form *in vivo* upon reaction of hydrazines with hemoglobin and myoglobin. For example, the erythrocyte aggregates called "Heinz bodies"[4] result from the *in vivo* reaction of phenylhydrazine with hemoglobin.

Because protoporphyrin is asymmetrically substituted at the periphery, eight isomers can result upon N-substitution of these macrocycles. The isomers are identified by the pyrrole ring to which the phenyl group is attached and are labeled A, B, C, and D in a counterclockwise fashion when protoporphyrin is oriented as shown in Figure 1. There are two distinct isomers for each pyrrole ring depending on whether the phenyl substituent is on the distal side or the proximal side of the porphyrin ring (in Figure 1, the porphyrin ring is oriented so that the distal side is *up*). We have investigated only the isomers with the phenyl attached on the distal side of the porphyrin macrocycle. The four distal isomers are obtained when phenylhydrazine reacts with myoglobin because the phenylhydrazine has access to only the distal side of the porphyrin; the protein limits access to the proximal side. Determination of the subset of isomers that result from the phenylhydrazine reaction with various heme proteins provides a useful way to map the accessible regions of the molecular surface of the heme groups.[5]

N-substituted porphyrins are interesting in their own right because of their novel structural conformation. There is an asymmetric distortion from planarity of the macrocycle resulting from addition of the pyrrole phenyl. Porphyrin planarity, which can also be affected by protein interactions, may influence the chemical and electron-transfer properties of tetrapyrroles contained in proteins such as methylreductase and the photosynthetic reaction center. The reported crystal structure of $Zn^{II}(Cl)$-*N*-phenyltetraphenylporphyrin) (ZnNPhTPP) reveals that the substituted pyrrole ring of this macrocycle is tilted with respect to the mean porphyrin plane by 42°.[6] Related ligand-insertion

*To whom correspondence should be addressed.
† Sandia National Laboratories.
‡ University of New Mexico.
§ University of California.

(1) Lavallee, D. K. *The Chemistry and Biochemistry of N-Substituted Porphyrins*; VCH Publishers: New York, 1987.
(2) Ortiz de Montellano, P. R.; Kunze, K. L.; Mico, B. A. *Mol. Pharmacol.* **1980**, *18*, 602.
(3) Kunze, K. L.; Ortiz de Montellano, P. R. *J. Am. Chem. Soc.* **1981**, *103*, 4225.
(4) (a) Heinz, R. *Virchows Arch. Pathol. Anat. Physiol. Klin. Med.* **1890**, *122*, 112. (b) Hoppe-Seylor, G. *Z. Physiol. Chem.* **1885**, *9*, 34.
(5) (a) Samokyszyn, V. M.; Ortiz de Montellano, P. R. *Biochemistry* **1991**, *30*, 11646. (b) Swanson, B. A.; Dutton, D. R.; Yang, C. S.; Ortiz de Montellano, P. R. *J. Biol. Chem.* **1991**, *266*, 19258. (c) Tuck, S. F.; Peterson, J. A.; Ortiz de Montellano, P. R. *J. Biol. Chem.* **1991**, *267*, 5614. (d) Tuck, S. F.; Aoyama, Y.; Yoshida, Y.; Ortiz de Montellano, P. R. *J. Biol. Chem.* **1992**, *267*, 13175. (e) Tuck, S. F.; Ortiz de Montellano, P. R. *Biochemistry* **1992**, *31*, 6911.
(6) Kuila, D.; Lavallee, D. K.; Schauer, C. K.; Anderson, O. P. *J. Am. Chem. Soc.* **1984**, *106*, 448.

0020-1669/93/1332-3153$04.00/0

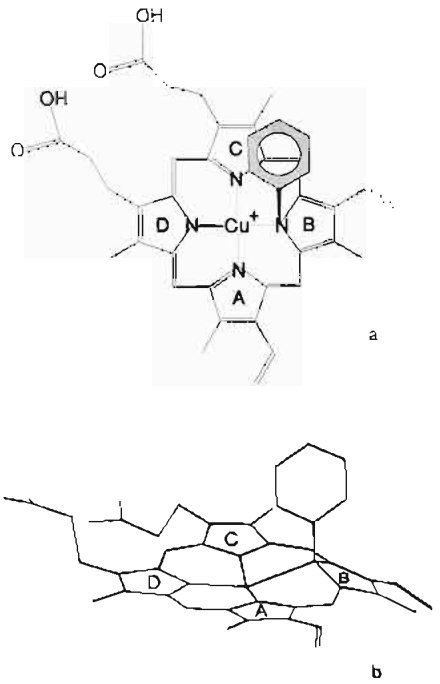

Figure 1. The Cu–*N*-phenylprotoporphyrin macrocycle: (a) computer drawing of a CuNPhPPDME; (b) energy-minimized structure of CuNPhPPDME. Placement of the N-substituent above or below the porphyrin ring gives respectively four distal or four proximal isomers.

complexes of tetraphenylporphyrins have also been reported.[7] Insertion of a ligand into the metal–nitrogen bond of one pyrrole ring causes this pyrrole ring to be tilted out of the mean porphyrin plane by 46.4°, while the dihedral angles between the plane of the four nitrogen atoms and the planes of the other three pyrrole rings are only 13.3, 5.9, and 3.6°.[7]

We have obtained resonance Raman and UV–visible absorption spectra of the isomers of two *N*-phenylprotoporphyrin metal derivatives. Dual-channel resonance Raman spectroscopy was used to obtain spectra of a single distal isomer (C) of Zn^{II}(Cl)-(*N*-phenylprotoporphyrin IX dimethyl ester) (ZnNPhPPDME) and, for comparison, phenyl-free Zn(protoporphyrin IX dimethyl ester) (ZnPPDME). We also obtained Raman spectra of all four distal isomers of Cu^{II}(*N*-phenylprotoporphyrin IX dimethyl ester) (CuNPhPPDME) and phenyl-free Cu^{II}(protoporphyrin IX dimethyl ester) (CuPPDME). These spectra provide useful structural information about the conformational differences between the protoporphyrins and their *N*-phenyl derivatives. In particular, the tilting of the substituted pyrrole ring leads to a decrease in the porphyrin π-conjugation, which in turn causes a decrease in the frequency of the structure-sensitive Raman vibrational modes. The spectra also can be used to identify the *N*-phenyl isomers of protoporphyrin and to elucidate the conformational differences between them. UV–visible absorption spectra and Raman spectra were also used to follow photochemical changes occurring in the Zn porphyrins during laser irradiation.

Molecular mechanics calculations were used to determine differences in the structure of the isomers and to assess the effects of different vinyl group orientations on the energetics. The calculations also aid in interpretation of the spectroscopic results. The crystal structure of ZnNPhTPP was first modeled to test the accuracy of the force field, and then energy-optimization calculations were carried out for various isomers and conformers of Cu^{II}(Cl)(*N*-phenylprotoporphyrin (CuNPhPP). Calculated structures were similar to structures reported[6,8-10] for N-substituted porphyrin with the major distortion from planarity occurring for the N-substituted pyrrole ring. Finally, the molecular mechanics calculations suggest that the spectral characteristics are a result of electronic effects rather than kinematic effects.

Materials and Methods

Synthesis of the Four Distal Regioisomers of Cu^{II}(*N*-phenylprotoporphyrin IX dimethyl ester). Phenylhydrazine hydrochloride (Aldrich) was recrystallized from ethanol and stored in the dark. Copper(II) acetate was from Mallinckrodt, and horse heart myoglobin was purchased from Sigma. All solvents used for HPLC and spectrophotometric analyses were HPLC grade. Electronic absorption spectra were obtained on a Hewlett-Packard 8450A diode-array spectrophotometer. Preparative HPLC was performed on a system consisting of a Hewlett-Packard 9153C controller, a Hewlett-Packard 1040A diode-array detector, and two Beckman Model 110A pumps.

The four CuNPhPP distal isomers were prepared by incubation of horse heart myoglobin with phenylhydrazine.[11] Myoglobin (300 mg) in 60 mL of water was reacted with sufficient (5 mM) phenylhydrazine hydrochloride to shift the Soret band from 408 to 430 nm. The solution was then added to 600 mL of 5% (vol/vol) sulfuric acid in acetonitrile, and the mixture was allowed to sit for 2 h at room temperature. The resulting green solution was concentrated by rotary evaporation, 500 mL of 5% (vol/vol) sulfuric acid in water was added, and the mixture was extracted with ethyl acetate. The combined organic extracts were evaporated to dryness; however, if an oil formed, it was redissolved in a small volume of 5% (vol/vol) sulfuric acid in water and extracted with dichloromethane. The four *N*-phenylprotoporphyrin isomers were purified using a Whatman semipreparative column (25 × 1 cm) packed with Partisil 10 ODS-3. The isomers were eluted isocratically for 30 min with a solution that consisted of 85% A (6:4:1 methanol:water:glacial acetic acid) and 15% B (10:1 methanol:glacial acetic acid), followed by 100% B for 5 min. The column was monitored at 410 nm. Each of the four isomers was collected, with the unresolved areas between peaks separately collected and rechromatographed using the same solvent system. The four isomers were rechromatographed to ensure high purity. Each purified isomer was esterified in 300 mL of 5% (vol/vol) sulfuric acid in methanol for 24 h at room temperature. Two volumes of water were then added, and the solution was extracted immediately with dichloromethane. The solvent was removed to dryness from the combined extracts by rotary evaporation. The esterified adducts were purified using the same HPLC system as before, but using 80% A and 20% B. The Cu(II) complexes were made by dissolving each adduct in a small amount of chloroform and adding aliquots of $Cu(acetate)_2$ dissolved in methanol. Chelation was monitored by UV–visible absorbance shifts. The solutions were then washed with water before the organic layer was blown down to a solid. The zinc complexes were prepared by dissolving the adducts in CH_2Cl_2 (2 mL) and adding approximately 100 μL of a 90 mM zinc acetate in methanol solution while complex formation was monitored at 440 nm. The zinc complexes were then purified by HPLC using the same solvent as used to purify the parent dimethyl esters. Each isomer was immediately taken to dryness on a rotary evaporator because the zinc complexes are labile.

Spectroscopic Techniques. Resonance Raman spectra of pairs of the N-substituted PPDME regioisomers were obtained simultaneously using a partitioned Raman cell and a dual-channel Raman spectrometer described elsewhere.[12] The 413.1-nm line from a Krypton ion laser (Coherent, Inc.) was the exciting source, and the scattered light was collected at 90° to the direction of propagation and polarization of the incident laser light. The Raman cell was rotated at 50 Hz. This allowed the samples in the two compartments to be probed alternately by the laser radiation and also prevented sample heating. Simultaneous collection of the spectra of the two samples in this fashion eliminates errors that result from variations in instrument response and grating positioning.

Samples were dissolved in methanol, and 150-μL aliquots were added to the two separate compartments of the cell. Laser power was 100 mW at the sample, and sample concentrations were in the range 1×10^{-4} to 1×10^{-5} M. Spectra of isomers A, C, and D of CuNPhPPDME were all obtained simultaneously with isomer B because this isomer was the most plentiful. In addition, polarized spectra for N-substituted isomer B and CuPPDME were obtained by attaching parallel and perpendicular polarizing filters to the partitioned cell, one on each side.

The Raman spectra were acquired and stored on an HP9000-375 computer (Hewlett Packard) and were simulated using a nonlinear least-

(7) Chottard, G.; Mansuy, D.; Callot, H. J. *Inorg. Chem.* **1983**, *22*, 362.
(8) Lavallee, D. K.; Anderson, O. P. *J. Am. Chem. Soc.* **1982**, *104*, 4708.
(9) Anderson, O. P.; Kopelove, A. B.; Lavallee, D. K. *Inorg. Chem.* **1980**, *19*, 2101.
(10) Callot, H. J.; Chevrier, B.; Weiss, R. *J. Am. Chem. Soc.* **1978**, *100*, 4733.
(11) Swanson, B. A.; Ortiz de Montellano, P. R. *J. Am. Chem. Soc.* **1991**, *113*, 8146.
(12) Shelnutt, J. A. *J. Phys. Chem.* **1983**, *87*, 605.

squares program.[13] The position of the peak maximum, the peak intensity, and the line width of up to eight lines (1000 data points) served as the parameters that were varied to obtain Lorentzian curve fits.[13] Also, the linear baseline was allowed to slope as well as vary vertically. Frequencies of the CuNPhPPDME regioisomers and CuPPDME were obtained from the peak maxima as revealed by the Lorentzian line shapes obtained from the curve fitting routine. The frequencies from the three resulting spectra of isomer B were averaged, and the frequencies of isomers A, C, and D were given with respect to the isomer B frequencies. Depolarization ratios were calculated using the peak maxima from curve fits of the parallel and perpendicular spectra.

Photochemical modification was observed only in ZnNPhPPDME (see Results section). For the Cu(II) derivative, porphyrin photodegradation was not observed during the 5–10 20-min scans of the spectrum. Sample integrity was monitored by UV–visible spectroscopy before and after the Raman spectrum was obtained and by examination of selected 20-min scans of the Raman spectrum obtained during signal averaging. UV–visible spectra were taken using a Perkin-Elmer Model 330 spectrophotometer.

Molecular Modeling Methods. Calculations were performed on a Personal Iris 4D35 workstation. Energy-optimized Cu^{II}(*N*-phenylprotoporphyrin) structures were obtained using BIOGRAF software (Molecular Simulations, Inc.), which utilizes a conjugate-gradient minimization technique with a force field that we have defined[14] on the basis of a normal-coordinate analysis of NiOEP,[15] the X-ray crystal structure of NiOEP,[16] and the Dreiding force field.[17] This force field was then modified[18] slightly for Cu and Zn using the X-ray crystal data for copper(II) octaethylporphyrin (CuOEP)[19] and zinc(II) tetrakis(4-pyridyl)porphyrin pyridine (Zn(py)TPyP).[20] The total energy was calculated as the sum of the bond stretching, bond bending (angle), torsion, inversion (or improper torsion term), electrostatic, and van der Waals energies. The electrostatic potential energy terms due to partial charges assigned to the atoms were found to have only a small effect on the structures and were neglected in the reported results. All isomers and conformers were energy-minimized using a convergence criterion of 0.001 (kcal/mol)/Å for the root-mean-square (rms) force.

Initially, the crystal structure of ZnNPhTPP[6] was modeled in order to obtain the parameters necessary to fit the distorted core geometry of N-substituted porphyrins. We found that only the M–N(s) bond required attention. The equilibrium bond distance and force constant for the Zn–N(s) bond were 3.070 Å (1.0 Å greater than the Zn–N (unsubstituted nitrogen) equilibrium bond distance of 2.070 Å) and 200 kcal-mol^{-1}/Å (42 kcal-mol^{-1}/Å less than the force constant used for the remaining three Zn–N bonds), respectively. The distal isomers of CuNPhPP were then constructed and energy-minimized. The equilibrium Cu–N(s) bond distance was also set at 1.0 Å longer than the usual Cu–N equilibrium bond distance of 1.970 Å (the force constant was 200 kcal-mol^{-1}/Å). The other Cu–N bonds (unsubstituted nitrogens) retained a force constant of 242 kcal-mol^{-1}/Å.

A subset of conformers for each of the A–D isomers exist which differ in the orientation of the vinyl substituents on the C_β (pyrrole β-carbon) atoms at the 2- and 4-positions. There are eight vinyl conformers: the vinyl groups can be rotated so that they point either toward the adjacent C_β atom or the C_m (meso bridging carbon). Also, since the interactions with the C_β and C_m substituents prevent an in-plane vinyl orientation, the vinyl groups must be directed out of the porphyrin plane toward either the distal side or the proximal side. A convenient method for naming the isomers and conformers is as follows. The name consists of six letters where the first letter indicates the isomer (A, B, C, D) and the second identifies which side of the protoporphyrin the phenyl group is on (P = proximal, D = distal). The third and fourth letters (P, D) refer to the out-of-plane conformation of vinyls 2 and 4, respectively. The fifth and sixth letters identify the in-plane conformation of vinyls 2 and 4, respectively (pointing toward the C_β atom (B) or toward the C_m proton (M)). For example, ADDDBB refers to a conformer of isomer A in which the phenyl group and both vinyls point toward the distal side of the porphyrin macrocycle and vinyls 2 and 4 are both oriented toward the C_β atoms.

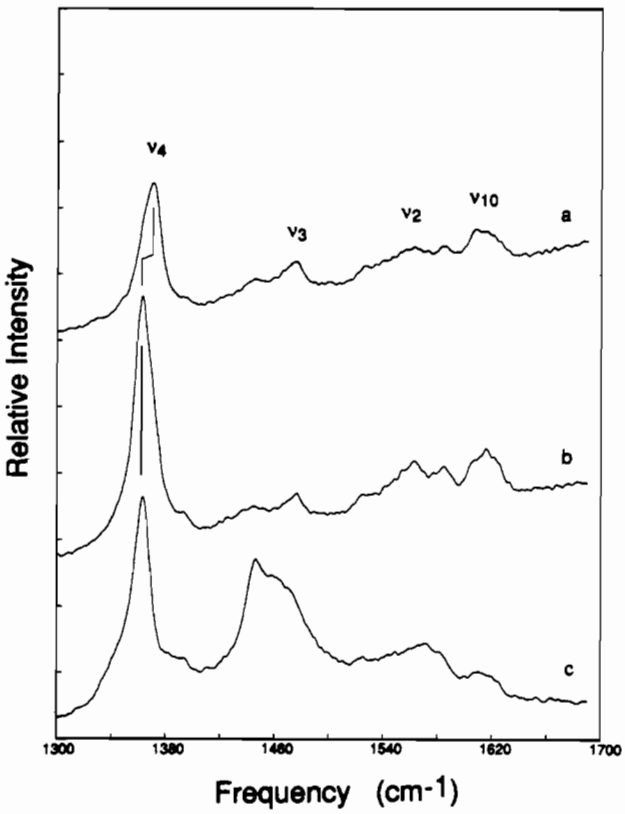

Figure 2. Resonance Raman spectra of (a) ZnNPhPPDME after 1 scan (20 min), and (b) ZnNPhPPDME after 2 scans (40 min), and (c) ZnPPDME after 1 scan. The excitation wavelength is 413 nm. The solvent is methanol. The structure-sensitive modes are labeled. Note the shift of ν_4 in the photoproduct to the same frequency as ν_4 in ZnPPDME.

The energy-minimized structures of the isomers (and their conformers) of CuNPhPP were analyzed to obtain bond distances, angles, dihedral angles (torsions), and the substituted pyrrole tilt. The tilt of the substituted pyrrole ring with respect to the porphyrin plane was obtained using two methods. In the first method, the pyrrole tilt was obtained by using the torsion of the C_α–C_m bond, or the $C_\alpha C_m$–$C_\alpha C_\beta$ dihedral angle. Two dihedral angles, one on each side of the substituted pyrrole ring, were averaged to give an estimate of the amount of pyrrole tilt. In the second method, the angle between the average plane of the porphyrin and the plane of the substituted pyrrole ring was used. First, a planar porphyrin template was matched to the protoporphyrin (using 16 atom pairs including N, C_α, C_m). The average plane of the porphyrin was then defined by the three nitrogen atoms (from the template) that were matched to the three unsubstituted nitrogens of the protoporphyrin. The plane of the substituted pyrrole ring was defined by simply chosing three of the five atoms comprising it (the substituted nitrogen, N(s), and the two C_β atoms).

Results

Spectroscopic Studies. Resonance Raman spectra of ZnNPhPPDME isomer C and ZnPPDME are shown in Figure 2. The Raman spectra after one scan (spectrum a; at 20 min) and after two scans (spectrum b; at 40 min) are compared with the spectrum of ZnPPDME (spectrum c). Because of the significant amount of photodegradation of ZnNPhPPDME isomer C, Raman studies of the other isomers were not attempted.

Table I contains UV–visible absorption data for the Zn(II) and Cu(II) derivatives of NPhPPDME. In general, the absorption bands of N-substituted porphyrins are red-shifted on the order of 10 nm from the bands of corresponding non-N-substituted

(13) Stump, R. F.; Deanin, G. G.; Oliver, J. M.; Shelnutt, J. A. *Biophys. J.* **1987**, *51*, 605.
(14) Shelnutt, J. A.; Medforth, C. J.; Berber, M. D.; Barkigia, K. M.; Smith, K. M. *J. Am. Chem. Soc.* **1991**, *113*, 4077.
(15) (a) Abe, M.; Kitagawa, T.; Kyogoku, Y. *J. Chem. Phys.* **1978**, *69*, 4526. (b) Kitagawa, T.; Abe, M.; Ogoshi, H., *J. Chem. Phys.* **1978**, *69*, 4516. (c) Li, X.-Y.; Czernuszewicz, R. S.; Kincaid, J. R.; Spiro, T. G. *J. Am. Chem. Soc.* **1989**, *111*, 7012. (d) Li, X.-Y.; Czernuszewicz, R. S.; Kincaid, J. R.; Stein, P.; Spiro, T. G. *J. Phys. Chem.* **1990**, *94*, 47.
(16) Brennan, T. D.; Scheidt, W. R.; Shelnutt, *J. Am. Chem. Soc.* **1988**, *110*, 3919.
(17) Mayo, S. L.; Olafson, B. D.; Goddard, W. A., III *J. Phys. Chem.* **1990**, *94*, 8897.
(18) Sparks, L. D.; Medforth, C. M.; Park, M.-S.; Chamberlain, J. R.; Ondrias, M. R.; Senge, M. O.; Smith, K. M.; Shelnutt, J. A. *J. Am. Chem. Soc.* **1993**, *115*, 581.
(19) Pak, R.; Scheidt, W. R. *Acta Crystallogr.* **1991**, *C47*, 431.
(20) Collins, D. M.; Hoard, J. L. *J. Am. Chem. Soc.* **1970**, *92*, 3761.

Table I. UV–Visible Absorption Maxima (nm) for $Cu^{II}(Cl)$(protoporphyrin dimethyl ester) (CuPPDME) and the $Cu^{II}(Cl)$(*N*-phenylprotoporphyrin dimethyl ester) Isomers (X = A, B, C, D) in Chloroform and for ZnPPDME and the Zn *N*-phenyl Isomers in Methanol

porphyrin	γ^a	β^a	α^a	
CuPPDME	405	534	571	
CuNPhPPDME				
A	436	542	610	
B	434	542	606	
C	430	538	602	
D	432	538	602	
ZnPPDME	414	544	583	
	(414)	(544)	(582)	
ZnNPhPPDME				
A	428	544	602	644
B	438	550	608	646
C	428	542	600	642
	(414)	(545)	(582)	
D	429	542	601	
HNPhB[b]	416	560, 579	604, 622	

[a] UV–visible data in parentheses were obtained *after* laser irradiation. [b] NPhPPDME isomer B free base in chloroform.

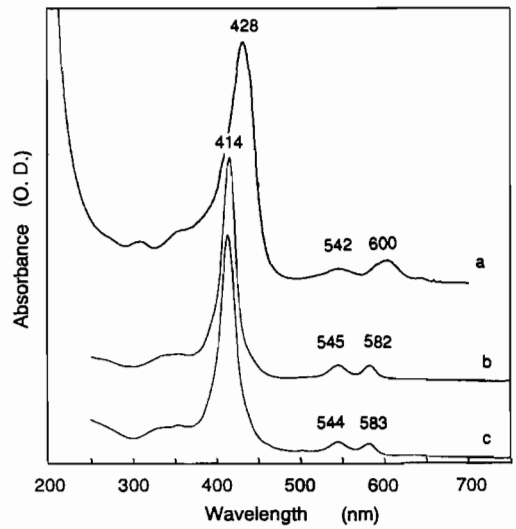

Figure 3. UV–visible spectra of (a) ZnNPhPPDME isomer C, (b) the photoproduct of isomer C, and (c) ZnPPDME. The solvent is methanol. The similarity between spectrum a and spectrum c suggests that the phenyl group is lost upon laser irradiation.

porphyrins.[1,6] Absorption band maxima of ZnPPDME and all ZnNPhPPDME isomers are given. Additionally, data for spectra of ZnNPhPPDME isomer C and ZnPPDME obtained after laser irradiation are listed. Also shown in Table I are the band maxima of the free base of isomer B; its UV–visible spectrum was obtained in chloroform whereas all other spectra were obtained in methanol. Figure 3 shows the UV–visible absorption spectra of ZnNPhPPDME isomer C (spectrum a), its photoproduct (spectrum b), and ZnPPDME (spectrum c). Note the similarity between the photoproduct (after Raman) of isomer C and ZnPPDME.

Resonance Raman spectra of the *N*-phenyl derivatives of CuPPDME (in methanol) are shown in Figure 4. Unlike the case of the ZnNPhPPDME derivatives, there was no photodegradation observed for the CuNPhPPDME derivatives upon laser irradiation. The spectrum of CuPPDME (in carbon disulfide; CuPPDME is not soluble in methanol) is also shown for comparison. Raman mode assignments are based on those for NiOEP[15] and NiPP.[21,22] Also, polarization studies were carried out for CuPPDME and CuNPhPPDME isomer B to aid in assigning some modes. The important Raman modes for the four CuNPhPPDME isomers, NiPPDME (in carbon tetrachloride[22] and in carbon disulfide), and CuPPDME (in carbon disulfide) are given in Table II. Note the similarity between the Raman spectra of NiPPDME taken in carbon tetrachloride and carbon disulfide. There are no significant changes in the Raman modes that can be attributed to the different solvents used.

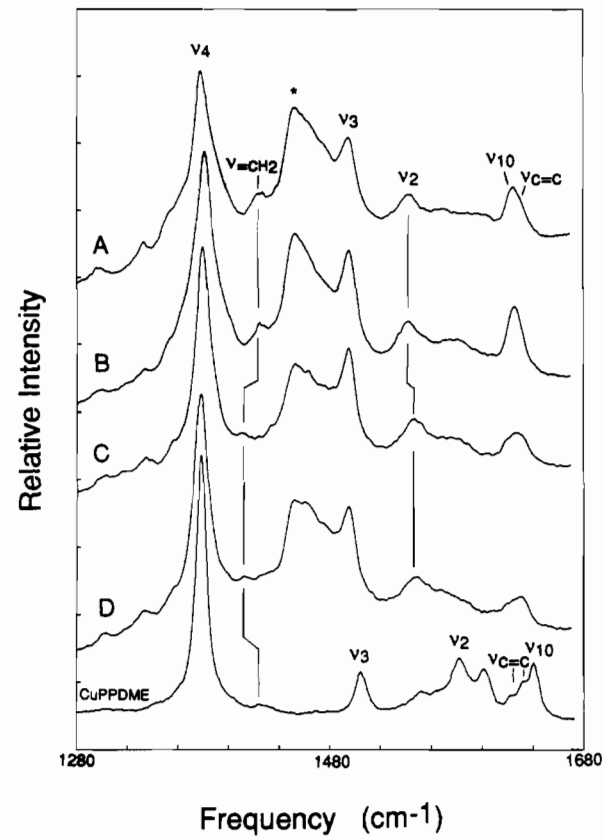

Figure 4. Resonance Raman spectra of the distal regioisomers of CuNPhPPDME in methanol and of CuPPDME in carbon disulfide. The excitation wavelength is 413 nm. Solvent peaks are marked with an asterisk. The structure-sensitive modes and some vinyl modes are labeled.

UV–visible data for the four CuNPhPPDME isomers and CuPPDME in chloroform are listed in Table I. Large red shifts are observed for the *N*-phenyl isomers relative to CuPPDME. Absorption spectra of CuNPhPPDME isomers A–D are similar although those for isomers A and B vary significantly with respect to those for isomers C and D. The γ, β, and α electronic transitions of isomers A/B are observed at slightly higher wavelengths than those of isomers C/D. Specifically, the average difference between isomers A/B and C/D for the γ, β, and α bands are 4, 4, and 6 nm, respectively. UV–visible spectra of the CuNPhPPDME regioisomers were also obtained in methanol (not listed). Again, bands for isomers A/B are at slightly higher wavelengths than those for isomers C/D (γ, β, and α bands differ by 6, 2, and 3 nm). Smaller spectral differences are noted between isomers A and B and between isomers C and D.

Molecular Energy-Optimization Calculations. Table III shows a comparison of the calculated structure of $Zn^{II}(Cl)$(*N*-phenyltetraphenylporphyrin) (ZnNPhTPP) to the crystal structure.[6] Parameters for the crystal that did not appear in the original paper[6] were obtained by using BIOGRAF software to enter the coordinates into the computer and analyze the structure. The experimental and calculated ZnNPhTPP structures were least-squares matched for the N, C_m, C_α, and C_β atoms of the porphyrin ring to obtain an rms difference of 0.15 Å for 24 coordinate pairs (Figure 5). Although ZnTPP (not shown) has a planar conformation, ZnNPhTPP is asymmetrically distorted from planarity. This distortion is most evident in the tilt of the N-substituted pyrrole ring (as measured by the $C_\alpha C_m$–$C_\alpha C_\beta$ dihedral angle or

(21) Kushmeider, K. *Analysis of Symmetry Lowering Effects on the Vibrational Spectra of Metalloporphyrins*; Dissertation, Princeton, 1991.

(22) Choi, S.; Spiro, T. G.; Langry, K. C.; Smith, K. M. *J. Am. Chem. Soc.* **1982**, *104*, 4337.

Table II. Raman Frequencies (cm^{-1}) and Depolarization Ratios for $Cu^{II}(Cl)$(protoporphyrin dimethyl ester) the $Cu^{II}(Cl)$(*N*-phenylprotoporphyrin dimethyl ester) Isomers, and NiPPDME

	CuNPhPPDME isomers (methanol)						
assign[a]	A	B	C	D	CuPPDME (CS_2)	NiPPDME (CS_2)	NiPPDME[b] (CCl_4)
ν_{21}, $\delta(C_m—H)$							1305 ap
δ(CH═)	**1296**	**1297**	**1303**	**1302**	**1301**	**1301**	**1305 p**
δ_s(═CH_2(2))	**1332**	**1332**	**1333**	**1332**	**1345**	**1345**	**1343 ap**
$\nu_4(C_\alpha—N)$	1377	1381 p	1379	1377	1376 p	1381	1381 p
$\nu_{20}(C_\alpha—N)$	1389	1394 ap					1399 ap
$\nu_{29}(C_\alpha—C_\beta)$							1401 dp
δ_s(═CH_2(1))	**1423**	**1425 dp**	**1404**	**1410**	**1431**	**1431**	**1434 dp**
$\nu_3(C_\alpha—C_m)$	1495	1495 p	1495	1495	1502 p	1520	1519 p
$\nu_2(C_\beta—C_\beta)$	1542	1540 p	1547	1547	1581 p	1591	1593 p
$\nu_{19}(C_\alpha—C_m)$	1570	1579	1578	1578			1603 ap
$\nu_{10}(C_\alpha—C_m)$	1623	1624 dp	1622	1623	1639 dp	1657	1655 dp
ν(C═C(1))	**1630**	**1629 p**	**1631**	**1632**	**1630 p**	**1633**	**1634 p**
					1620 p		

[a] Mode assignments from refs 15, 21, and 22. [b] From ref 22.

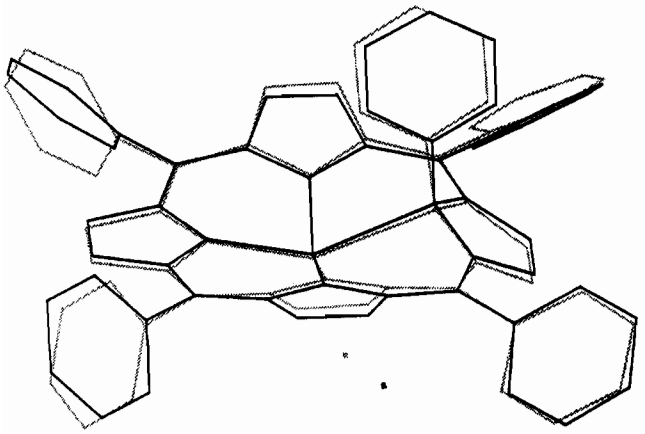

Figure 5. Matched structures of calculated ZnNPhTPP (gray) and the crystal structure[6] (solid lines). Note the close match of the phenyl group orientation and the core geometry.

by the angle between the average plane of the porphyrin and the plane of the substituted pyrrole ring, "planes" in Table III). Distortion of the porphyrin macrocycle from planarity is also measured using the N–Zn–N angle (across the porphyrin). In the calculated structure, the N–Zn–N angle (adjacent to the substituted pyrrole ring) is 10° larger (180° for the N–Zn–N angle indicates a planar macrocycle), and the substituted pyrrole tilts slightly less. The orientation of the *N*-phenyl substituent is given by the *N*-phenyl angle in Table III. The phenyl group is calculated to be nearly parallel with the N–Zn–N bond axis but is offset by 4° in the X-ray structure.

Tables IV–VI contain data for CuPP and for the isomers and conformers of CuNPhPP. Results for the lowest energy conformers of the A–D isomers are given first in the Tables IV and VI. The lowest energy conformers generally have both of the vinyl groups rotated toward the adjacent C_β atom, as can be seen by comparison of the structures of the in-plane vinyl conformers for isomer A at the bottom of Table IV. For these in-plane vinyl conformers, designated ADDDXX (where X = M, B), the vinyl groups were both held in the distal (D) orientation but rotated so that they were pointed toward either the C_m proton (M) or the C_β atom (B). For the out-of-plane conformers, designated ADXXBB (where X = D, P), the vinyl groups were held so that they pointed toward the C_β atom but rotated so that they were oriented up (distal) or down (proximal). Table V gives a comparison of the Cu–N bond lengths and selected angles for CuPP and the isomers of CuNPhPP.

The effects of N-substitution are reflected in several structural parameters of the porphyrin macrocycle. Not surprisingly, the N-substituted porphyrins are more highly strained than the planar non-N-substituted CuPP, in which the macrocycle geometry is planar with essentially no tilt or twist of the pyrrole rings. Energetically, the CuNPhPP's are 127 kcal/mol higher in energy than the CuPP's (Table IV). Approximately 32 kcal/mol of this is associated with the Cu–N(s) bond in the CuNPhPP's. This leaves a 95 kcal/mol difference in energy between CuPP and CuNPhPP. Most of this difference is due to torsion energy, and the rest is derived from the bonds, van der Waals forces, and angles. Structurally, strain is evident in the Cu–N bond length, which is 2.00 Å for all four bonds in CuPP but which increases for CuNPhPP to 2.41 Å for Cu–N(s) (see Table V). Also, the four C_α–N–C_α angles in CuPP are 106.1° but, in CuNPhPP, the C_α–N(s)–C_α angle is calculated to be 3° less and the other three C_α–N–C_α angles in CuNPhPP are slightly greater than those in CuPP (Table V). The N–Cu–N angle measures the amount of bending (as in a saddle distortion)[14] of the macrocycle. In CuPP, the average of the two N–Cu–N angles is 176°, but in CuNPhPP this angle is 160°.

The conformers differing in the orientation of the vinyl groups were investigated in detail, and the results for CuNPhPP isomer A are given in Tables IV and VI. In general, the structure of CuNPhPP was not significantly affected by the changes in vinyl group orientation. However, for each conformer of CuNPhPP isomer A, there is a significant difference in the total energy (0.2–3.3 kcal/mol) due to the vinyl orientations. Generally, lower total energies are observed when the vinyl substituents are oriented toward the C_β atom instead of the C_m proton.

Table III. Comparison of Crystal (xtal) and Calculated (calc) Data for $Zn^{II}(Cl)$(*N*-phenyltetraphenylporphyrin)[a]

	xtal[b]	calc
	Bond Lengths (Å)	
Zn–N(s)	2.49	2.50
Zn–N(o)	2.02	2.04
Zn–N(a)	2.10	2.07
	Bond Angles (deg)	
C_α–N(s)–C_α	106.8	104.6
C_α–N(o)–C_α	108.0	107.6
C_α–N(a)–C_α	105.2	107.2
C_α–C_m–C_α(a)	123.5	121.4
C_α–C_m–C_α(o)	124.1	122.3
N–Zn–N(s)	144.1	143.6
N–Zn–N(a)	141.3	151.0
	Substituted Pyrrole Tilt (deg)	
$C_\alpha C_m$–$C_\alpha C_\beta$	28.4	27.8
planes[c]	36.6	34.4
	N-Phenyl Angle (deg)	
N(o)N(s)–C_1C_2	4.2	0.1

[a] N(s) = substituted nitrogen, N(o) = the pyrrole nitrogen opposite to N(s), N(a) = the pyrrole nitrogens that are adjacent to N(s). C_1 and C_2 are on the phenyl substituent. [b] From ref 6. [c] "Planes" are defined in Table VI and in the text.

Discussion

The N-substituted porphyrins provide a unique opportunity to obtain a basic understanding of distortions of metalloporphyrins

Table IV. Energies (kcal/mol) of the Low-Energy Conformers of Cu^{II}NPhPP and the In-Plane and Out-Of-Plane Vinyl Conformers of Cu^{II}NPhPP

isomer[a]	total	bonds	angles	torsions	inversions	constr[b]	vdWs[c]
			CuPP				
	85.8	8.0	82.2	5.0	0.2		39.8
			CuNPhPP (Lowest Energy Conformers)				
ADPPBB	213.2	34.3	91.8	54.7	0.5	31.6	51.0
BDPPBB	213.7	34.2	91.9	54.9	0.5	31.7	51.1
CDDPBB	213.5	34.0	91.8	54.8	0.6	31.9	50.9
DDPDBB	212.8	34.1	91.7	54.5	0.6	31.8	50.7
			CuNPhPP (Out-of-Plane Vinyl Conformers for Isomer A)				
ADDDBB	214.4	34.3	91.6	54.9	0.6	31.7	51.8
ADDPBB	213.4	34.2	91.3	55.0	0.6	31.6	51.3
ADPDBB	214.1	34.4	92.2	54.4	0.5	31.6	51.6
ADPPBB	213.2	34.3	91.8	54.7	0.5	31.6	51.0
			CuNPhPP (In-Plane Vinyl Conformers for Isomer A)				
ADDDBM	215.2	34.0	90.9	58.1	0.7	31.7	50.5
ADDDMB	214.3	34.2	91.7	56.9	0.7	31.4	50.0
ADDDMM	216.5	34.0	91.4	60.0	0.9	31.5	49.4

[a] Conformer names are defined in the text. [b] The Cu–N(s) (phenyl-substituted nitrogen) equilibrium bond distance was constrained to 2.97 Å. The force constant was set at 200 kcal/mol. [c] Energy due to nonbonding interactions (van der Waals forces).

Table V. Angles and Copper–Nitrogen Bond Distances of CuPP and the Low-Energy Conformers of Cu^{II}NPhPP[a,b]

	CuPP	ADPPBB	BDPPBB	CDDPBB	DDPDBB
		Bond Lengths (Å)			
Cu–N(s)		2.408	2.407	2.405	2.406
Cu–N(o)		1.965	1.965	1.969	1.967
Cu–N(a)		1.995	1.996	1.997	1.996
average	2.002	2.091	2.091	2.092	2.091
		Bond Angles (deg)			
C_α–N(s)–C_α		103.4	103.4	103.3	103.4
C_α–N(o)–C_α		106.6	106.6	106.7	106.7
C_α–N(a)–C_α		106.3	106.4	106.4	106.3
av	106.1	105.7	105.7	105.7	105.7
C_α–C_m–C_α(a)		126.6	126.7	126.1	126.0
C_α–C_m–C_α(o)		125.3	125.2	125.8	125.9
av	125.4	125.9	126.0	126.0	126.0
N–Cu–N(s)		154.9	155.2	155.4	155.4
N–Cu–N(a)		164.2	163.7	163.5	163.9
av	176.2	159.5	159.5	159.5	159.7

[a] Conformer names are defined in the text. [b] N(s) = substituted nitrogen, N(o) = the pyrrole nitrogen opposite to N(s), N(a) = the pyrrole nitrogens that are adjacent to N(s).

Table VI. Dihedral Angles (deg) of Cu^{II}NPhPP In-Plane and Out-of-Plane Vinyl Conformers

	vinyl dihedral angles					pyrrole tilt	
isomer[a]	vinyl 2	vinyl 4	av	diff	phenyl angle[b] MN–CC	dihed[c]	planes[d]
			CuPP				
	14.7	14.9	14.8	0.2		1.4	
			CuNPhPP (Lowest Energy Conformers)				
ADPPBB	12.7	14.1	13.4	1.4	2.2	17.9	28.8
BDPPBB	16.1	12.8	14.4	3.2	0.2	17.8	26.7
CDDPBB	13.1	14.2	14.6	3.1	1.8	18.6	27.4
DDPDBB	14.1	13.7	13.9	0.4	0.6	18.4	27.2
			CuNPhPP (Out-of-Plane Vinyl Conformers)				
ADDDBB	14.8	15.7	15.2	1.0	0.5	20.1	27.1
ADDPBB	13.9	14.4	14.2	0.5	0.4	19.7	27.9
ADPDBB	12.9	15.4	14.2	2.5	2.2	18.2	26.0
ADPPBB	12.7	14.1	13.4	1.4	2.2	17.9	26.8
			CuNPhPP (In-Plane Vinyl Conformers)				
ADDDBM	13.6	24.6	19.1	11.0	0.7	19.7	28.5
ADDDMB	23.5	13.7	18.6	9.9	1.1	15.3	25.1
ADDDMM	21.0	24.3	22.6	3.3	1.6	16.4	26.8

[a] As in Table V. [b] Where the C's are phenyl carbons. This dihedral gives the plane of the phenyl ring with respect to the plane defined by the substituted nitrogen, the metal, and the nitrogen opposite the substituted nitrogen. [c] This dihedral ($C_\alpha C_m C_\alpha C_\beta$) gives the orientation of the substituted pyrrole ring with respect to the porphyrin plane. [d] The angle between the pyrrole plane (defined as the N, C_β, and C_β atoms of the substituted pyrrole ring) and the plane of the porphyrin macrocycle (defined by the C_α, C_m, and N atoms of the other three pyrrole rings).

from planarity. The particular distortion of the N-substituted porphyrins is not typical of other porphyrins, which exhibit either the common ruffled conformation in which the pyrrole rings are twisted about the metal–nitrogen bonds or a saddle conformation in which two opposite pyrrole rings are tilted up and the other two are tilted down. The saddle-type distortion has been noted in a series of MOATPP's,[14,18] and the ruffled distortion is found in the tetragonal NiOEP crystal.[23] Recently, structures in which a mixture of saddle and ruffled conformations are apparent were predicted using molecular mechanics calculations in certain sterically crowded metalloporphyrins;[24] even so, all pyrrole rings are symmetrically distorted. In contrast, the distortion from planarity caused by N-substitution occurs primarily in only one pyrrole ring. We have used spectroscopic techniques and molecular modeling calculations to investigate this type of nonplanar distortion of the porphyrin.

We also address the problem of identifying the isomers of N-phenyl- protoporphyrin using resonance Raman spectroscopy. Specific Raman modes that are perturbed by this type of distortion and that distinguish each of the isomers are identified. The N-substituted porphyrins have not been the subject of vibrational spectroscopic studies.[1] However, X-ray crystallography has been used extensively to determine the degree of distortion of several different N-substituted porphyrins. These include chloro-*N*-methyl-5,10,15,20-tetraphenylporphyrin complexed with Mn(II),[25] Fe(II),[9] Co(II),[26] and Zn(II),[27] the Co(II) complex of chloro-*N*-((ethylcarbonyl)methyl)octaethylporphyrin,[28] and Zn^{II}NPhTPP.[6] Some free-base structures have also been reported.[8] These structures indicate that there are several well-defined structural features of the N-substituted porphyrins that differentiate them from the non-N-substituted porphyrins. The most striking of these is the tilt of the substituted pyrrole ring. The resulting disruption of the π-conjugation of the porphyrin macrocycle should be as identifiable in the Raman spectrum as it is in the UV–visible absorption spectrum. The hybridization of the nitrogen atom (sp^2 in normal metalloporphyrins) becomes sp^3-like upon N-substitution. This change in hybridization influences the degree to which the metal and nitrogen atoms interact with each other and may affect the π-conjugation of the macrocycle as well.[1] As

(23) Meyer, E. F., Jr. *Acta Crystallogr.* **1972**, *B28*, 2162.
(24) Sparks, L. D.; Shelnutt, J. A. Unpublished results.
(25) Anderson, O. P.; Lavallee, D. K. *Inorg. Chem.* **1977**, *16*, 1634.
(26) Anderson, O. P.; Lavallee, D. K. *J. Am. Chem. Soc.* **1976**, *98*, 4670.
(27) Lavallee, D. K.; Anderson, O. P.; Kopelove, A. B. *J. Am. Chem. Soc.* **1978**, *100*, 3025.
(28) Goldberg, D. E.; Thomas, K. M. *J. Am. Chem. Soc.* **1976**, *98*, 913.

a result, the M–N bond of the N-substituted pyrrole ring is longer than the M–N bonds of the unsubstituted nitrogens. These electronic structure differences should be apparent in the frequencies of the structure-sensitive lines in the Raman spectrum. Thus, besides providing a means of identifying the four isomers, the Raman spectra should provide additional information about the electronic structure and conformation of the N-substituted porphyrins.

Raman Spectroscopy. Resonance Raman spectroscopy is a useful tool for structural studies of the metalloporphyrins; the most informative Raman modes are typically the structure-sensitive modes, ν_4, ν_3, ν_2, and ν_{10}. As might be expected, these modes are most useful for the comparison of N-substituted with non-N-substituted protoporphyrins. While complete normal-coordinate analyses for NiOEP[15] and NiTPP[29] (D_{4h} symmetry) are available, the analysis of resonance Raman spectra is especially difficult when asymmetric molecules like protoporphyrin are studied. However, the Raman spectra of many metalloporphyrins of lower symmetry (C_{4v}, C_{2v}, and D_{2d} for example) can be analyzed, to first order, by analogy to NiOEP or NiTPP normal coordinates. For nickel protoporphyrin the normal-coordinate labels still apply for modes with frequencies above 1300 cm^{-1} in spite of the lower symmetry[21,22] although the resonance Raman spectrum is more complex because the E_u out-of-plane modes and the vinyl substituent modes become Raman active. The complexity is most apparent for the low-frequency region, which is strongly influenced by the peripheral substituents and by vibrations involving the metal ion. For the N-substituted protoporphyrins, this region is quite complicated but reveals larger differences between isomers than does the high-frequency region.

Spectra of Copper(II) Protoporphyrin IX Dimethyl Ester and Copper(II) *N*-Phenylprotoporphyrin IX Dimethyl Ester. The modes of CuPPDME (in carbon disulfide) are assigned on the basis of the normal-coordinate analysis that is derived from the experimental data of NiPPDME (in carbon tetrachloride).[21,22] Our spectrum of NiPPDME in carbon disulfide (not shown) is comparable to that of NiPPDME in carbon tetrachloride[22] (Table II). A comparison of the skeletal Raman modes of NiPPDME and CuPPDME reveals that the frequencies of CuPPDME are lower than those of NiPPDME. In particular, the modes ν_4, ν_3, ν_2, and ν_{10} downshift by 5, 18, 10, and 18 cm^{-1}, respectively (Table II). The low Raman frequencies for CuPPDME are not surprising since the porphyrin skeletal modes are known to be sensitive to metal core size.[18,30] The larger Cu(II) ion would be expected to expand the core and thus decrease the frequencies of the marker lines. In contrast, most of the vinyl modes are located at the same frequency in both Cu- and NiPPDME. The only exception is ν(C=C), the mode at 1633 cm^{-1} in NiPPDME which is only 3 cm^{-1} lower in CuPPDME.

A comparison of the N-substituted CuPPDME isomers with CuPPDME reveals large differences in the structure-sensitive high-frequency modes. Except for ν_4, these modes downshift considerably for the isomers of CuNPhPPDME relative to CuPPDME. The distortion from planarity caused by N-substitution disrupts the π-conjugation of the protoporphyrin macrocycle, hence weakening the skeletal bonds and lowering the Raman frequencies. This decrease in frequency of the structure-sensitive modes is common to all nonplanar distortion modes that have been investigated thus far.[7,14,18] Most dramatic are the downshifts in the porphyrin modes ν_2 and ν_{10} in the CuNPhPPDME isomers, which are shifted respectively by −37 and −16 cm^{-1} with respect to those modes in CuPPDME.

There have been no previous Raman studies on N-substituted porphyrins. However, Chottard et al.[7] have examined metalloporphyrins with a bridging ligand inserted between the metal and a pyrrole nitrogen. They compared $Fe^{III}[C{=}C(p\text{-}ClHC_6H_4)_2]TPP$ to $Fe^{III}(Cl)TPP$, and $Ni^{II}(CHCOOC_2H_5)TPP$ was compared to $Ni^{II}TPP$. The ligand-inserted Fe(III) and Ni(II) complexes are analogous to our *N*-phenyl species in that they have one pyrrole ring tilted out of the mean plane (a plane through the four pyrrole nitrogen atoms). The distortion results in a decrease in π-conjugation within the porphyrin ring, weaker π–π bonds in the porphyrin, and lowered vibrational frequencies. For example, it was found[7] that ν_2 and ν_{10} for the ligand-inserted TPP's shifted by −17 and −13 cm^{-1} for the Fe(III) derivative and by −31 and −23 cm^{-1} for the Ni(II) derivative with respect to their unmodified TPP counterparts. The anomalously polarized (ap) mode, ν_{19}, at 1515 and 1546 cm^{-1} for Fe^{III}- and $Ni^{II}TPP$, respectively, was also found to shift in spectra of the insertion derivatives by −5 and −29 cm^{-1}. The occurrence of new but weak vibrational modes below 1000 cm^{-1}, dispersion of the depolarization ratios, and frequency lowering of the two highest porphyrinic vibrational modes were found to be characteristic features of the resonance Raman spectra of these ligand-inserted metalloporphyrins.

The Raman modes that arise from, or that are coupled to, the vibrations of the vinyl groups are also informative in comparing the N-substituted with unmodified protoporphyrin. For CuPPDME, the vinyl double bond stretch, ν(C=C), is observed at 1630 cm^{-1}. The symmetric vinyl CH_2 scissor deformation, $\delta_s(=CH_2)$, is split into $\delta_s(=CH_2(1))$ and $\delta_s(=CH_2(2))$ because of interaction with porphyrin skeletal modes. For NiPPDME specifically, the 1343-cm^{-1} anomalously polarized (ap) mode is coupled to the skeletal mode at 1399 cm^{-1} (ν_{20}, ap) and the depolarized (dp) vinyl mode at 1434 cm^{-1} is coupled to the skeletal mode at 1401 cm^{-1} (ν_{29}, dp).[22] For CuPPDME, this split results in two peaks at 1345 and 1431 cm^{-1}. For CuNPhPPDME $\delta_s(=CH_2(1))$ is at 1332 cm^{-1} and $\delta_s(=CH_2(2))$ is at ~1424 cm^{-1} for isomers A and B and at 1404 and 1410 cm^{-1} for isomers C and D. It is likely that these vinyl modes in the spectrum of CuNPhPPDME interact with the same skeletal modes as those in the spectra of Ni- and CuPPDME.

The structure-sensitive skeletal modes, however, do not vary greatly between the N-substituted isomers of CuNPhPPDME. Distinctions between the regioisomers of CuNPhPPDME originate from the Raman modes that involve the vinyl substituents and the C_β–C_β bond stretch of the porphyrin. The C_β atoms are perturbed the most by peripheral substitution of the pyrrole rings. The Raman modes that are associated with the vinyl substituents sometimes couple with the porphyrin skeletal modes as a result of additional π delocalization onto the vinyl groups. In fact, a recent normal-coordinate analysis[21] shows a slight coupling between the vinyl stretch and modes having a large C_β–C_β stretching component. For example, the vinyl C=C stretch and the skeletal mode, ν_2, couple, resulting in an enhanced vinyl mode.[21]

The most significant differences in the resonance Raman spectra of CuNPhPPDME isomers are evident in the vinyl modes. These modes differ depending on the pair of isomers examined; A and B are similar and C and D are similar but large differences between these pairs occur. In isomers A and B the *N*-phenyl substituent is bound to the pyrrole rings that have the vinyl groups attached at the 2- and 4-C_β atoms; in isomers C and D, the phenyl ring is on the pyrrole rings that lack the vinyl substituents. Thus, frequency differences for vinyl modes are expected between these pairs of isomers. For example, δ(CH=) is at 1297 cm^{-1} for isomers A/B and at 1303 cm^{-1} for C/D. The vinyl double bond stretch, ν(C=C), is less than 10 cm^{-1} from ν_{10} in each isomer. These modes are collectively broader, and less intense, for isomers C/D, whereas, for isomers A/B, the spectral features including ν_{10} and ν(C=C) are narrower and more intense. However, the opposite is true for Raman lines underlying ν_4: isomers A/B each have a broad ν_4 line and those of C/D are more similar to that of CuPPDME, i.e., narrower. Also, ν_{20} has gained intensity in the A/B spectra but is not observed in the C/D spectra. The differences between isomers A/B and C/D are also observed in

(29) Li, X.-Y.; Czernuszewicz, R. S.; Kincaid, J. R.; Su, Y. O.; Spiro, T. G. *J. Phys. Chem.* **1990**, *94*, 31.

(30) (a) Spaulding, L. D.; Chang, C. C.; Yu, N.-T.; Felton, R. H. *J. Am. Chem. Soc.* **1975**, *97*, 2517. (b) Spiro, T. G.; Stong, J. D.; Stein, P. *J. Am. Chem. Soc.* **1979**, *101*, 2648.

the splitting of the vinyl mode $\delta_s(=CH_2)$ to give $\delta_s(=CH_2(1))$ and $\delta_s(=CH_2(2))$. Here, $\delta_s(=CH_2(2))$ is the same for isomers A–D, but $\delta_s(=CH_2(1))$ varies from 1404 to 1425 cm^{-1} for the four isomers. The split between $\delta_s(=CH_2(1))$ and $\delta_s(=CH_2(2))$ is larger for isomers C/D by $\sim$13 cm^{-1}. This difference is probably the result of $\delta_s(=CH_2)$ for isomers A/B interacting differently with porphyrin skeletal modes than $\delta_s(=CH_2)$ for isomers C/D. Finally, there is a 6-cm^{-1} difference in ν_2 between A/B and C/D. The skeletal mode ν_2 is expected to shift substantially more than other skeletal modes, such as ν_4 and ν_3, because it consists mainly of the C_β–C_β stretch which is in close proximity and coupled to the vinyl C=C mode.

Spectra of Zinc(II) Protoporphyrin IX Dimethyl Ester and Zinc(II) *N*-Phenylprotoporphyrin IX Dimethyl Ester. The resonance Raman spectra of ZnNPhPPDME isomer C (spectra a and b) and ZnPPDME (spectrum c) (shown in Figure 2) clearly indicate that photochemical modification of the porphyrin occurs. For ZnNPhPPDME isomer C, the first scan (spectrum a) shows the oxidation-state marker line ν_4 at 1376 cm^{-1} with a shoulder at about 1368 cm^{-1}. In the second 20-min scan (spectrum b), the shoulder dominates with only slight evidence of a peak remaining at 1376 cm^{-1}. Other less quantifiable changes in the spectrum are also observed, indicating that ZnNPhPPDME isomer C undergoes a structural change as a result of photochemistry. For example, a mode near 1614 cm^{-1} in the vicinity of the vinyl stretch changes position.

The similarity of the Raman spectrum of the photoproduct (spectrum b; Figure 2) and that of ZnPPDME suggests that the phenyl ring of ZnNPhPPDME isomer C is photochemically removed. This is shown most obviously by the structure-sensitive mode, ν_4, of the ZnNPhPPDME isomer C photoproduct which shifts to the same frequency as ν_4 for ZnPPDME. Additional, less severe modifications of the molecular structure may also be occurring. The loss of the phenyl substituent is confirmed, as shown in Figure 3 by the similarity of the absorption spectra of the photoproduct of isomer C (spectrum b) and ZnPPDME (spectrum c). For ZnNPhPPDME isomer C before photodecomposition, the γ, β, and α bands are at 428, 542, and 600 nm, respectively (spectrum a). After photodecomposition, the ZnNPhPPDME isomer C photoproduct shows γ, β, and α bands at 414, 545, and 582 nm, respectively. Hence, the bands of the photoproduct and ZnPPDME are almost identical.

ZnPPDME also exhibits photochemical changes, although the changes occur on a much longer time scale. While UV–visible spectra (not shown) taken before and after laser irradiation show little evidence of photodecomposition, the Raman spectra (not shown) are more revealing of the photochemical changes. After the first 20-min scan of ZnPPDME (in methanol), a weak shoulder appears at $\sim$1350 cm^{-1}. By the second scan, the shoulder is more prominent, indicating slow photodecompostion of ZnPPDME. The extent of photodegradation after 40 min is much less than that incurred in the *N*-phenyl derivative (ZnNPhPPDME isomer C). Examination of the sample after the Raman spectra were obtained showed that bleaching had also occurred. Raman spectra of ZnPPDME in two solvents, methanol and carbon disulfide (not shown), indicate that the porphyrin is more stable in methanol.

Molecular Energy-Optimization Calculations. Molecular mechanics calculations aid in the interpretation of resonance Raman spectra and in assessing the effects of different vinyl group orientations on the energetics of the isomers and conformers of CuNPhPP. In this study, we have used the crystal structure of $Zn^{II}(Cl)$(*N*-phenyltetraphenylporphyrin) (ZnNPhTPP)[6] as a model for calculations of the N-substituted protoporphyrins. The molecular mechanics calculations, using a M–N(s) bond distance of 3.070 Å, yielded a structure that was surprisingly close to the crystal structure. The pyrrole tilt, as measured by the $C_\alpha C_m$–$C_\alpha C_\beta$ dihedral angle and by taking the angle between the average plane of the porphyrin and the plane of the substituted pyrrole ring was slightly underestimated in the calculation. The N–Zn–N(s) angle (see Table V) was also slightly underestimated, indicating that our calculated structure was slightly more planar than the crystal structure. A difference between the calculated and experimental structures for the N–Zn–N(a) angle (9.7°) is noted. The calculated structure is forced to be more planar perhaps because the nature of the substituted nitrogen (the altered hybridization due to N-substitution) was not taken into account in the calculation. In spite of these differences, the rms difference for the least-squares match (using 24 coordinate atom pairs; C_β, C_α, C_m, and N atoms) of the calculated and experimental structures of ZnNPhTPP is only 0.15 Å (Figure 5). This model was used in the energy-optimization calculations for the isomers of CuNPhPP.

There are obvious differences between N-substituted and unmodified porphyrins. Comparing CuNPhPP with CuPP (Tables IV–VI), CuPP is essentially planar, the Cu–N bond lengths are all similar, the N–Cu–N angle is close to 180°, and the pyrrole tilt as measured by the $C_\alpha C_m$–$C_\alpha C_\beta$ dihedral angle is only 1°. On the other hand, the CuNPhPP structures are highly distorted in an asymmetric fashion (Figure 1); the phenyl group pulls the nitrogen atom up out of the plane of the porphyrin, causing the familiar tilt of the substituted pyrrole down out of the porphyrin plane ($\sim$27°). Also, the Cu–N(s) bond is longer than the other three Cu–N bonds, as expected. The vinyl dihedral angle, which gives the deviation from planarity (with the pyrrole ring) of vinyl groups, is approximately the same for both vinyl groups (14.8°, Table VI) of CuPP. However, in the CuNPhPP's, the dihedral angles for vinyls 2 and 4 range from 12.7 to 16.1° (cf. below). The molecular mechanics calculations show only subtle structural differences between isomers A/B and C/D. For instance, for the N–Cu–N (opposite nitrogens) and C_α–C_m–C_α angles and the pyrrole tilt dihedral angle, the differences were only 0.2, 0.5, and 0.6°, respectively, between isomers A/B and C/D.

The effect of altering the vinyl group orientations on the conformation and energy of CuNPhPP was minimal. The dihedral angles (Table VI) of the vinyl substituents on the lowest energy conformers were also analyzed in detail. Vinyl 2 on isomer A and vinyl 4 on isomer B have similar vinyl dihedral angles (12.7 and 12.8°). The vinyls both point down or toward the proximal side of the porphyrin in the lowest energy structures of isomers A and B. For isomer B, vinyl 2 has the largest dihedral angle, which means that it is the farthest out of the pyrrole plane. Vinyl 4 for this isomer has one of the lowest dihedral angles. These differences can be explained using a proximity argument. In isomer B, vinyl 2 is on the C_β atom of ring A that is closest to the substituted pyrrole ring B. Vinyl 4 is on the tilted ring B and points in the same direction as the tilt. Also, vinyl 4 is sterically hindered by the neighboring methyl group, which may inhibit any further movement of the vinyl group out of the mean porphyrin plane. On isomer A, vinyl 2 has a small dihedral angle (12.7°) and the dihedral angle of vinyl 4 is larger (14.1°) but is still 2° less than that for vinyl 2 in isomer B (16.1°).

The trends in the vinyl dihedral angles of isomers C and D are slightly different from those of isomers A and B. When the phenyl group is on pyrrole ring C, vinyls 2 and 4 are oriented distal and proximal, respectively, and vinyl 2 is $\sim$1° closer to planarity than vinyl 4. This is because the N-substituted pyrrole ring is across the porphyrin from vinyl 2 but adjacent to vinyl 4. On isomer D, vinyls 2 and 4 are out of plane on the proximal and distal sides, respectively, and their dihedral angles are similar (14.1 and 13.7°). The dihedral angles for vinyls 2 and 4 are most similar in isomer D because vinyl 4 is across from the distorted pyrrole ring and vinyl 2 is on the C_β atom of pyrrole ring A that is farthest from the tilted ring D. In other words, for isomer D, the vinyls are farthest away from the N-substituted pyrrole ring and therefore less affected by it.

Energetically, the CuNPhPP's are destabilized with respect to CuPP by 127 kcal/mol. Most of this difference is evident in the torsion energy, which increases 11-fold upon N-substitution. The

other energies do not increase as drastically. For example, the bond energy for CuNPhPP (34 kcal/mol) is four times larger than that for CuPP (8 kcal/mol). On the other hand, the calculations show only subtle energy differences between isomers A/B and C/D. For example, although the total energies (Table IV) are similar for the four isomers, the energies due to van der Waals forces and bonds are each different by ~0.2 kcal/mol. Further, the energies of the four isomers of protoporphyrin (A–D) vary slightly depending upon which pyrrole ring is N-substituted. This variation in energy originates from the interaction of the phenyl with the pyrrole ring on which it resides and is also dependent upon the identity of the peripheral substituents that reside on that pyrrole ring. The energy of the protoporphyrins was also expected to be dependent upon the orientation of the two vinyl substituents because these groups are involved in the π-conjugation of the porphyrin macrocycle.

The conformers of CuNPhPP isomer A are also listed in Tables IV and VI. Although 16 conformers (which differ in the orientation of the two vinyl groups) are possible for each isomer, only a representative example of the extremes are given in Tables IV and VI. The out-of-plane vinyl conformers are significantly lower in total energy than the in-plane vinyl confromers (~1.3 kcal/mol). This difference is revealed mainly in the torsion energy: the average out-of-plane torsion energy versus the in-plane is 54.8 versus 57.5 kcal/mol. The energies due to bonds and van der Waals forces are slightly lower in the in-plane conformers. This result is not surprising because the vinyls (2 or 4 or both) are now pointing toward the C_m proton and away from the methyl groups, so that there is less steric interaction between the methyls and vinyls in the in-plane conformers. Strain between the methyl and vinyl groups is reflected in the vinyl dihedral angles of Table VI. Take, for example, the difference between the conformers ADDDBB and ADDDBM. The dihedral angles for vinyls 2 and 4 are 14.8 and 15.7° for ADDDBB, and those for ADDDBM are 13.6 and 24.6°. The only difference in the two structures is that vinyl 4 is twisted so that it points toward the C_m proton instead of toward the C_β methyl group. Note that in cases where the vinyl groups are oriented toward the C_m proton, the vinyl dihedral becomes large (21–25°) with respect to the vinyl dihedral angles of the out-of-plane conformers. When the vinyls point toward the C_m proton, there is less steric strain associated with the vinyl group and it deviates more from the plane of the pyrrole ring.

The changes in molecular geometry have bearing on the vibrational frequencies as a result of electronic or kinematic effects. The molecular mechanics calculations can be used qualitatively to assess whether the resonance Raman spectral characteristics of the vinyl groups are due to kinematic or electronic effects. The change in the force constant of a bond that is associated with the stretching motion of that bond is considered an electronic effect. A kinematic effect may be thought of as a change in the frequency of certain modes as a result of a change in geometry (movement of atoms) without reference to electronic effects (i.e. a change in the force constant of the bond contributing to the mode of interest). The vinyl modes of protoporphyrin display group frequencies; a kinematic effect would be apparent directly in these Raman modes. Further, a kinematic effect would be indicated in our calculations in the form of significant difference in the vinyl group orientation. In fact, the vinyl group orientations vary little between the isomers and conformers of CuNPhPP, indicating that the observed resonance Raman spectral characteristics are probably due to electronic effects instead.

Conclusions

Resonance Raman spectroscopy and molecular mechanics calculations give useful structural information about N-substituted porphyrins. Generally, for metalloporphyrins, the most useful Raman modes are the structure-sensitive modes, ν_4, ν_3, ν_2, and ν_{10}, and we have shown that these modes are very informative when the N-substituted porphyrins are compared to the unsubstituted porphyrins. For example, except for ν_4, these modes shifted to considerably lower frequencies for the CuNPhPPDME's relative to CuPPDME. These downshifts were a result of weakening of skeletal bonds due to the disrupted π-conjugation of the porphyrin macrocycle upon N-substitution. However, the structures of the *N*-phenyl isomers of CuPPDME (A–D) are not easily distinguished on the basis of the structure-sensitive Raman modes. For this purpose, the vinyl modes and the porphyrin modes that are coupled to the vinyl modes are more informative in that they *do* allow distinction between the isomers of CuNPhPPDME. The vinyl modes are resonance enhanced by π delocalization onto the vinyl groups and therefore show more significant changes when the phenyl substituent is placed on different pyrrole nitrogens of the protoporphyrin. Differences in the vinyl-dependent Raman modes are dependent upon whether the phenyl is directly substituted onto a pyrrole bearing a vinyl or not. That is, the vinyl modes of the A and B isomers are similar because the substituted pyrroles bear vinyl groups and C and D are similar because they do not bear vinyl substituents.

The question arises as to whether the vinyl differences are caused by kinematic or electronic effects. Using Zn^{II}NPhTPP as a model, we have shown that molecular mechanics calculations, using a force field that was based on a planar metalloporphyrin, are accurate. The effects of N-substitution were most prominent in the tilt of the substituted pyrrole and the Cu–N bond distances. Although there was a slight difference in total energy between isomers A/B and isomers C/D, there were no significant conformational differences apparent in our calculated structures. We therefore suggest that differences among the isomers in the vinyl Raman frequencies are electronic. That is, when the phenyl group is on either pyrrole ring A or B, the resulting nonplanar distortion disrupts the π-conjugation of that pyrrole ring with the rest of the macrocycle. Disruption in the π-conjugation of the macrocycle with pyrrole ring A or B influences the π-conjugation of the vinyl group with the pyrrole ring, giving shifts in the vinyl mode frequencies. These shifts are different from those observed when the phenyl substitution is on rings C and D, which have only an indirect effect on the π-conjugation of pyrroles A and B, to which the vinyls are conjugated.

Unlike the stable CuNPhPPDME isomers, ZnNPhPPDME isomer C underwent immediate photochemical modification upon laser irradiation. The resultant photoproduct has Raman and UV–visible spectra that are similar to those for ZnPPDME, suggesting that the phenyl ring of ZnNPhPPDME isomer C was photochemically removed.

Acknowledgment. Work performed at Sandia National Laboratories was supported by U.S. Department of Energy Contract DE-AC04-76DP000789 (J.A.S). Work at UCSF was supported by NIH Grant GM 25515 (P.R.O.d.M). L.D.S. acknowledges an Associated Western Universities graduate fellowship.